ADB103383

doc. 10

Some Surface Wave Modulation Mechanisms Relating to the JOWIP and SARSEX Observations

MITRE CORP MCLEAN VA

MAY 1986

Abstract

Large internal wave amplitudes were observed in the JOWIP and SARSEX experiments. These led to significant surface wave modulations, as observed directly and from radar observations. Modulation mechanisms are reviewed, including a two-step process by which longer wavelength waves modulate short waves. Some calculations are presented.

LIST OF TABLES

1.0 INTRODUCTION

Several experiments have been conducted to measure the modulation of surface waves by internal waves. The DREP (Defense Research Establishment Pacific) experiment in Bute Inlet and Georgia Straits was reported by Hughes and Grant.[1] A series of experiments were conducted jointly by DARPA and ONR during July-August, 1983, in Georgia Straits. The internal wave observations are described in the JOWIP Interim Report.[2] A third series of observations, sponsored by the ONR, were made in the New York Bight off the coast of Long Island in August-September, 1984. These are described in the SARSEX Interim Report.[3]

In both the JOWIP and SARSEX experiments in situ measurements were made of the internal wave and surface wave activity. In addition, L-band and X-band observations of the sea surface were conducted. In these experiments large amplitude internal waves, strong stratification, and thin mixed layers were encountered. This resulted in substantial surface wave modulation. Calculations of the expected modulation were made for JOWIP by the JHU/APL and TRW teams[2] and for SARSEX by the JHU/APL team.

For the JOWIP experiment the observed L-band modulations were larger than those calculated by factors of 2 to 10. The SARSEX

2.0 SURFACE WAVE RELAXATION MODEL

The surface current associated with the internal wave (IW) field is here assumed to have the form

$$\underline{U} = \hat{i}\, U_o\, h(Y). \qquad (2.1)$$

Here U_o is the peak surface current, $h(Y)$ is the IW current form factor, and we have taken the X-axis as the direction for IW propagation. In (2.1) we have written

$$Y = x - C_I t, \qquad (2.2)$$

where C_I is the IW phase velocity.

The radiative transport equation for the surface wave action density $F(\underline{k},\underline{x},t)$ is written as

$$\left[\frac{\partial}{\partial t} + \dot{\underline{x}} \cdot \nabla_x + \dot{\underline{k}} \cdot \nabla_k\right] F = S(\underline{k}, \underline{x}, t). \qquad (2.3)$$

Here

$$\dot{\underline{x}} = \nabla_k H, \ \dot{\underline{k}} = -\nabla_x H, \qquad (2.4)$$

and

$$H = \omega(k) + \underline{k} \cdot \underline{U} \qquad (2.5)$$

is the ray path "Hamiltonian". For gravity waves the frequency is

$$\omega(k) = (gk)^{1/2} \tag{2.6}$$

(Capillary waves will be discussed in Section 4.0) The quantity S in (2.3) includes effects of viscous damping, wind driven excitation, and nonlinear wave-wave interactions.

In a coordinate system in which the IW wave (2.1) is stationary, we may re-write (2.3) in the simpler form

$$[\dot{Y}\frac{\partial}{\partial Y} + \dot{k}_x \frac{\partial}{\partial k_x}]\, F(\underline{k},Y) = S(\underline{k},Y). \tag{2.7}$$

Now, equations (2.4) become

$$\dot{Y} = C(k)(\frac{k_x}{k}) - C_I + U(Y),$$

$$\dot{k}_y = 0,$$

$$\dot{k}_x = -k_x \frac{\partial U}{\partial Y}, \tag{2.8}$$

where $C(k) = d\omega/dk$ is the surface wave group velocity.

Hughes[9] has proposed an empirical model for S(k) that has frequently been used by other authors. As generalized by Phillips,[10] this has the form

$$S(\underline{k}, \underline{x}) = \beta_o(\underline{k})\, F[1 - (F/F_o)^m]. \qquad (2.9)$$

The quantity $F_o(k)$ is considered as the "equilibrium spectrum" to which S implies a tendency for F to relax. Hughes chose m = 1, whereas Phillips suggests that m = 2 or 3. In any case, if we assume that $|F - F_o| << F_o$, we obtain from (2.9) the linearized form

$$S(\underline{k},\underline{x},t) = -\beta(\underline{k})[F(\underline{k},\underline{x},t) - F_o(\underline{k})]. \qquad (2.10)$$

In this expression β appears as a relaxation rate. Hughes[9] and Phillips[10] adopt a model wind generation rate for β. Phillips, specifically, uses the semi-empirical expression given by Plant.[11]

The relaxation of a pattern of surface gravity waves was studied by Watson,[12] who obtained, in addition to the effects of wind and viscosity, a contribution to β from wave-wave interactions. This included both 3-wave and 4-wave couplings. The 3-wave interactions lead to a modest "smearing" of the wave spectrum. This 3-wave effect will not contribute significantly to (2.10) unless F is determined to great precision in the wave number $\underline{k}$. For the present applications it seems appropriate to omit this contribution to β. The 4-wave interactions do give a contribution, however, which at the higher wind speeds somewhat exceeds that from wind interaction.

We have chosen to model β by simply summing the contributions from viscosity, wind[11] and 4-wave interactions.[12] The result, expressed in terms of β^{-1} (in seconds) is shown as a function of k and wind speed V in Figure 2-1.

The very strong variation of β with wind speed V and wave number k, as indicated in Figure 2-1, suggests that there will be (k, V) regimes for which we can neglect S in (2.7) and others in which this term will be dominant. We illustrate this by quoting the familiar limits for a weak current U. Then we can treat

$$F' = F - F_o \tag{2.11}$$

as a small quantity. If we set S = 0 in (2.7), these results

$$F'(\underline{k},Y) \simeq \left\{\frac{U}{\left[C(k)\left(\frac{k_x}{k}\right) - C_I\right]}\right\} k_x \frac{\partial F_o}{\partial k_x} . \tag{2.12}$$

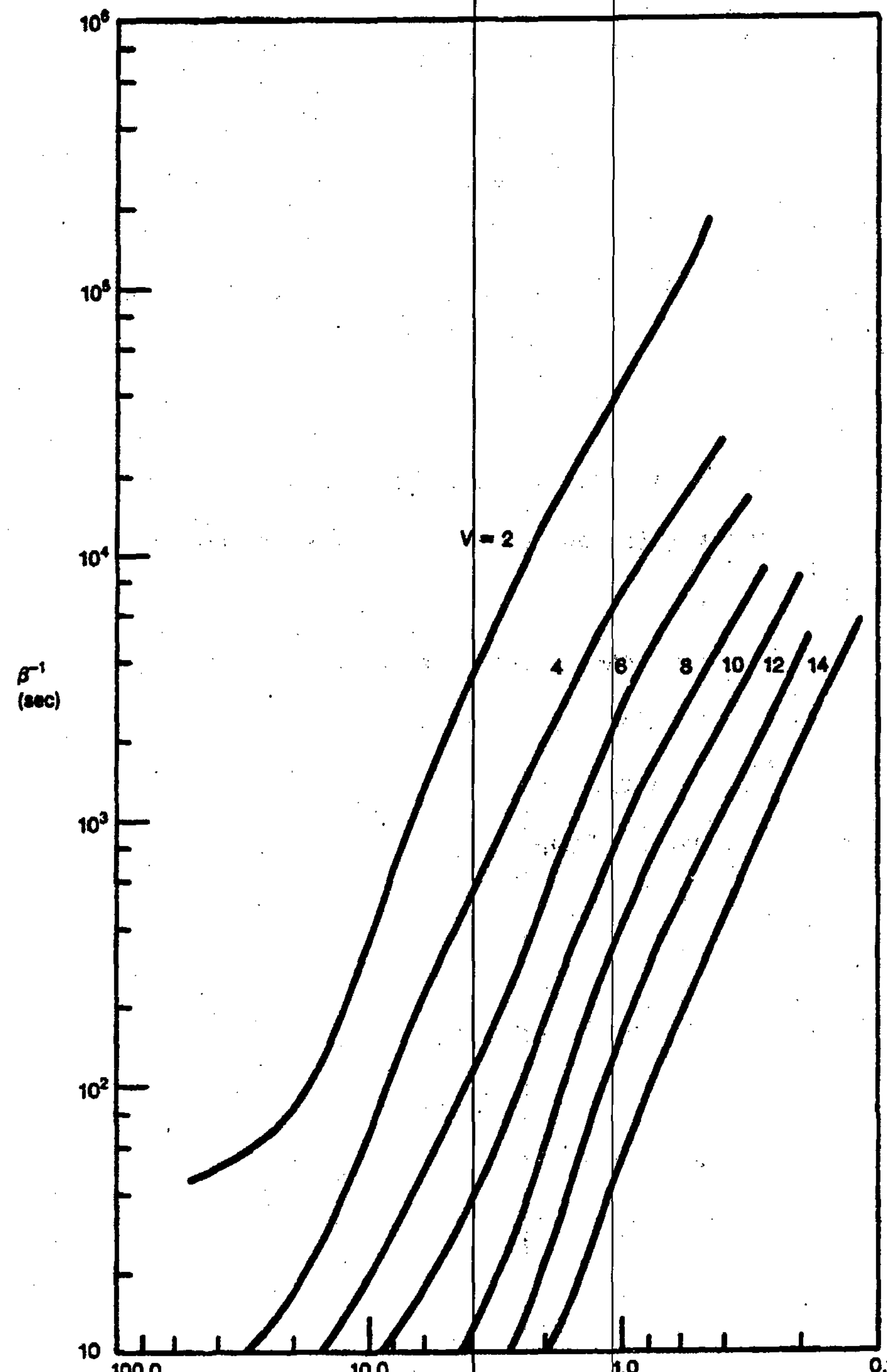

Figure 2-1. The surface wave relaxation time β^{-1} [see Equation (2.10)] is shown as a function of wavenumber k for several wind speeds. (V expressed in m/s.)

On the otherhand, in the limit of large β we find that

$$F'(k,Y) \cong \beta^{-1} \frac{\partial U}{\partial Y} \; k_x \frac{\partial F_o}{\partial k_x} . \tag{2.13}$$

For the case of wave "G2" reported from the SARSEX observations, we take

$\underset{\sim}{V}$ = (6 m/s, $\psi = 35^o$ = angle with respect to X-axis)

C_I = -0.5 m/s (propagation in negative X-direction)

U_o = 0.25 m/s

Np = 30 cph = peak Variala frequency

mixed layer thickness =10m.

$\Delta Y = \frac{300}{(2\pi)}$ = length scale

$\beta \cong 1.5 \text{ sec}^{-1}$, X-band

$\;\;\cong 0.1 \text{ sec}^{-1}$, L-band (2.14)

To apply this to (2.13), we write

$$M' = \frac{F'}{F_o} = -\left(\frac{\alpha}{\beta}\right) \frac{U}{\Delta Y}, \tag{2.15}$$

where

$$\alpha = -k_x \; \frac{\partial}{\partial k_x} \ln F_o . \tag{2.16}$$

In this report we shall take

$$\alpha = \frac{9}{2},$$

obtained from a Phillips spectrum with waves propagating in the X-direction. Application of the environmental conditions (2.14) to (2.15) gives

$$\begin{aligned} |M'| &\approx 0.02, \text{ X-band } (\lambda = 0.03\text{m}) \\ &\approx 0.2, \text{ L-band } (\lambda = 0.2\text{m}). \end{aligned} \tag{2.17}$$

If we take

$$\left|C(k)\left(\frac{kx}{k}\right) - C_I\right| = C_I,$$

(2.12) gives

$$|M'| \approx 2. \tag{2.18}$$

This is, of course, too large for the assumption that $|M'| << 1$, used in deriving (2.12).

We may estimate the wavelength regime in which it is valid to take $\beta = 0$ from the condition

$$\beta \leq \frac{C(k)}{2\pi\Delta Y}. \tag{2.19}$$

For a wind speed $V = 6$ m/s and $\Delta Y = 50$ m, this gives

$$k \leq 2.5 \text{ m}^{-1} \text{ or } \lambda \geq \frac{2\Pi}{k} = 2.5 \text{ m}. \tag{2.20}$$

Thus, for both L-band and X-band Bragg waves the limit (2.13) seems appropriate.

Comparison of (2.17) and (2.18) suggests the possible importance of the CW^2 mechanism. The longer gravity waves for which β may be taken as negligible are anticipated from (2.18) to have large modulation. If this is passed onto the Bragg waves, then (2.17) may represent a significant underestimate.

3.0 MODULATION IN THE REGIME FOR WHICH β IS SMALL

In this section we shall assume that it is valid to set S = 0 in (2.7). This equation then reads

$$[\dot{Y}\frac{\partial}{\partial Y} + \dot{k}_x \frac{\partial}{\partial k_x}] F = 0. \tag{3.1}$$

For a convenient model of the IW field, we take a semi-infinite wave train of the form [see (2.1)]

$$h(Y) = \frac{\cos(KY)}{[1 + \exp(-0.5\ KY)]}. \tag{3.2}$$

The ray equations (2.8) are to be integrated from a time t = 0 when $Y = Y_o$, $k_x = k_{xo}$, and $k_y = k_{yo}$. The initial position Y_o is so chosen that

$$KY_o \leq -3\pi, \tag{3.3}$$

which implies that

$$h(Yo) \cong 0. \tag{3.4}$$

Then, we can assume that

$$F\ (k_o,\ Y_o) = F_o\ (\underline{k}_o), \tag{3.5}$$

the "equilibrium" spectrum. Integration is carried to a time t_1 such that

$$2\pi < KY < 4\pi, \tag{3.6}$$

where $Y = Y(t_1)$ and $k_x = k_x(t_1)$. The action density at time t_1 is then obtained from (3.1) as

$$F\ (k,Y) = F_o\ (\underline{k}_o). \tag{3.7}$$

As a practical matter, (3.7) was evaluated by integrating the ray equations (2.8) backwards in time, starting at a prescribed Y and $\underline{k}$ at time t_1. Integration was carried back to a time such that (3.3) was valid and the resulting "initial" k_o was used to evaluate (3.7). The resulting gravity wave modulation is defined as

$$M(\underline{k},Y) = \frac{F(\underline{k},Y)}{F_o(k)}. \tag{3.8}$$

The corresponding modulation obtained from weak current perturbation theory is

$$M_{\text{pert}}\ (\underline{k},Y) = \frac{F'\ (\underline{k},Y)}{F_0\ (\underline{k})} + 1, \tag{3.9}$$

where F' is calculated using (2.12). Comparison of (3.8) and (3.9) permits us to specify the regime in which perturbation theory is valid.

To justify neglecting the relaxation term S in (3.1) we impose the condition that

$$\beta(k)\ \Delta t < 1, \tag{3.10}$$

where Δt is the average time for the phase point to travel a distance $\frac{2\pi}{k}$ in the integration of (2.8). We also, quite evidently, require that the phase point actually penetrate into the IW field to the point Y. In presenting our results, we have set

$$M\ (\underline{k},Y) = 0, \tag{3.11}$$

unless both of these conditions are satisfied. [Over most of the domain of our calculations these two conditions were roughly equivalent.]

For application to the present calculations we have chosen the "equilibrium" gravity wave spectrum to be of the form:

$$F_o(\underline{k}) = \left[\frac{g}{\omega(k)}\right] \underline{\Psi}_o(\underline{k}), \tag{3.12}$$

where the surface displacement spectrum is

$$\Psi_o(\underline{k}) = 0, \; k<k_W,$$

$$= \frac{\left(\frac{4x10^{-3}}{k^4}\right) \cos^s\left(\frac{\phi}{2}\right)}{L(s)}, \; k > k_W$$

$$k_W = \frac{g}{V^2},$$

$$s(k) = 15\left(\frac{k_W}{k}\right)^{5/4},$$

$$L(s) = \int_{-\pi}^{\pi} \cos^s\left(\frac{\phi}{2}\right) d\phi. \tag{3.13}$$

(See Tyler et al,[13] and Mitsuyasu et al.[14]) The quantity ϕ here is the angle between $\underline{k}$ and the wind velocity vector $\underline{V}$.

$$C_I = + 0.05 \text{ m/s}. \tag{3.16}$$

We call this SARSEX' and display the resulting modulation in Figure 3-2. The modulation, as calculated, is considerably enhanced with respect to that of Figure 3-1. We again anticipate that wave breaking may limit the actual modulation.

The variation of modulation with the phase of the IW is shown in Figure 3-3. The environmental conditions are those of SARSEX[1], with $\theta = 0°$.

The next set of environmental conditions considered are labelled as ENVEX1:

$$\begin{aligned}
&\underline{V} = (6 \text{ and } 3 \text{ m/s}, \psi = 0°)\\
&C_I = 0.33 \text{ m/s}\\
&U_o = 0.016 \text{ m/s}\\
&Np = 10 \text{ cph}\\
&\text{mixed layer thickness} = 10 \text{ m}\\
&\text{IW wavelength} = 160 \text{ m}
\end{aligned} \tag{3.17}$$

The IW eigenmodes where calculated in the WKB approximation for an exponential N-profile and the lowest mode was used. The resulting

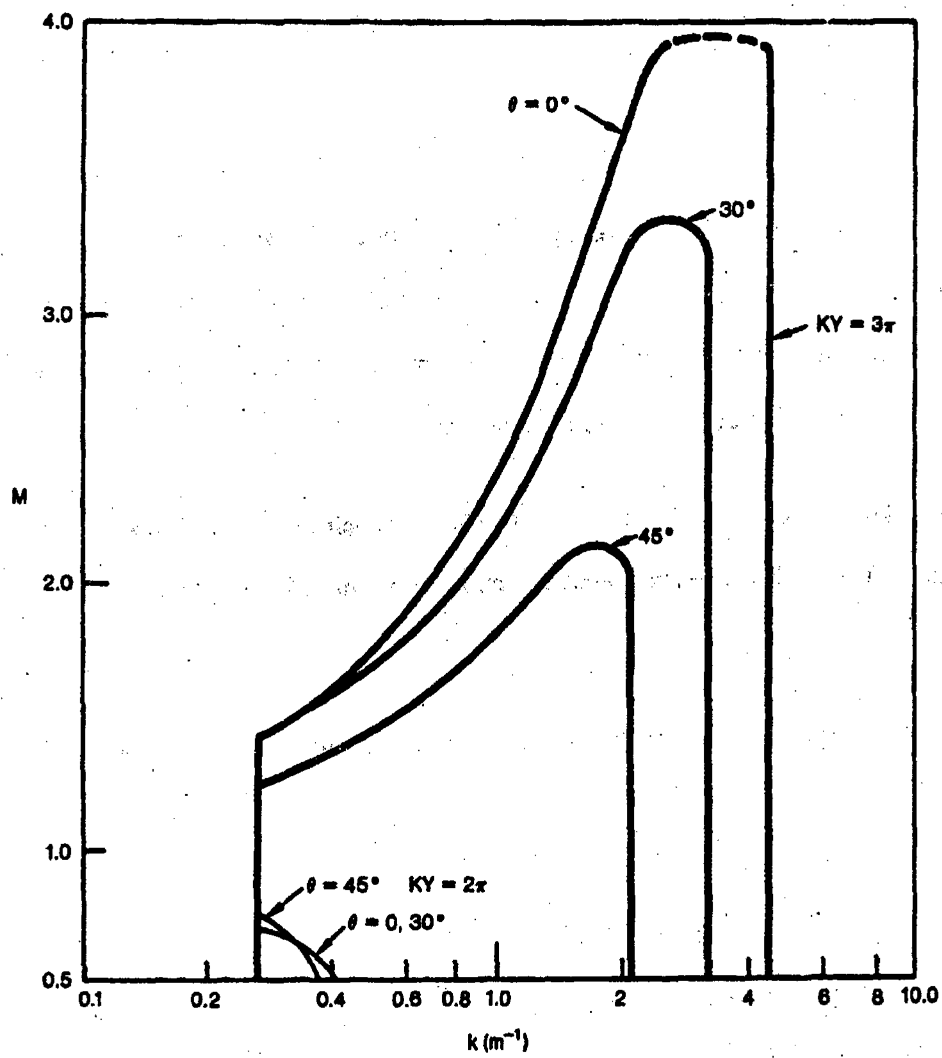

Figure 3-2. Surface wave modulation as predicted for conditions of the SARSEX I experiment. The environmental conditions are the same as those of Figure(3-1), except that the direction of propagation of the internal wave has been reversed.

modulation is shown in Figure 3-4 for $Y = \frac{3\pi}{K}$ (maximum modulation). The solid curves correspond to V = 6 m/s nd the dashed curves to V = 3 m/s.

The modulation is shown in Figure 3-5 for the same environmental conditions and $Y = \frac{3\pi}{K}$, but with IW propagation up-wind (C_I = -0.33 m/s). The substantial reduction of modulation for the up-wind case is again noted.

The final set of environmental conditions considered is labelled as ENVEX2:

$$\begin{aligned}
&\underline{V} = (6 \text{ and } 3 \text{ m/s}, \psi = 0°) \\
&C_I = 0.3 \text{ m/s} \\
&U_o = 0.03 \text{ m/s} \\
&Np = 15 \text{ cph} \\
&\text{mixed layer thickness} = 10 \text{ m} \\
&\text{IW wavelength} = 80 \text{ m.}
\end{aligned} \tag{3.18}$$

The lowest IW eigenmode for an exponential N-profile was again used.

We show the resulting modulation at $Y = \frac{3\pi}{K}$ in Figure 3-6. The direction of IW propagation is down-wind. The solid curves correspond to V = 6 m/s; the dashed curves correspond to V = 3 m/s.

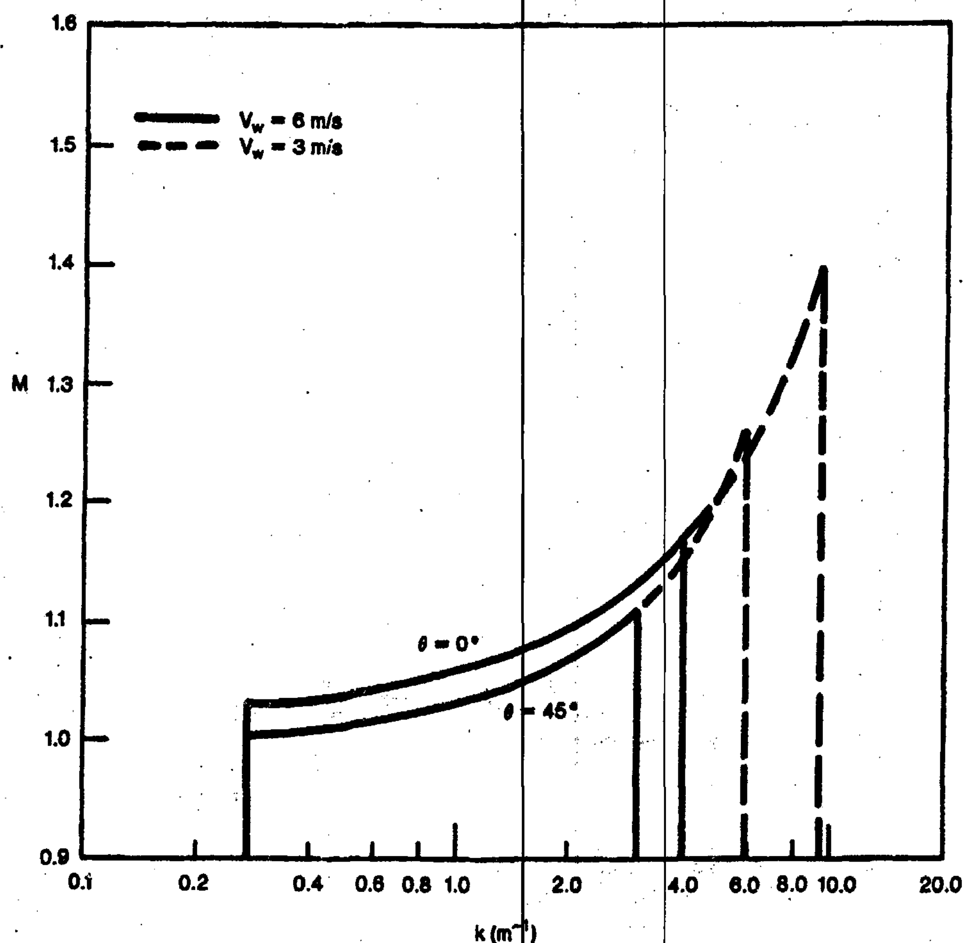

Figure 3-4. Surface wave modulation as predicted for the ENVEX1 "experiment," equation (3.17). The internal wave is propagation in the wind direction.

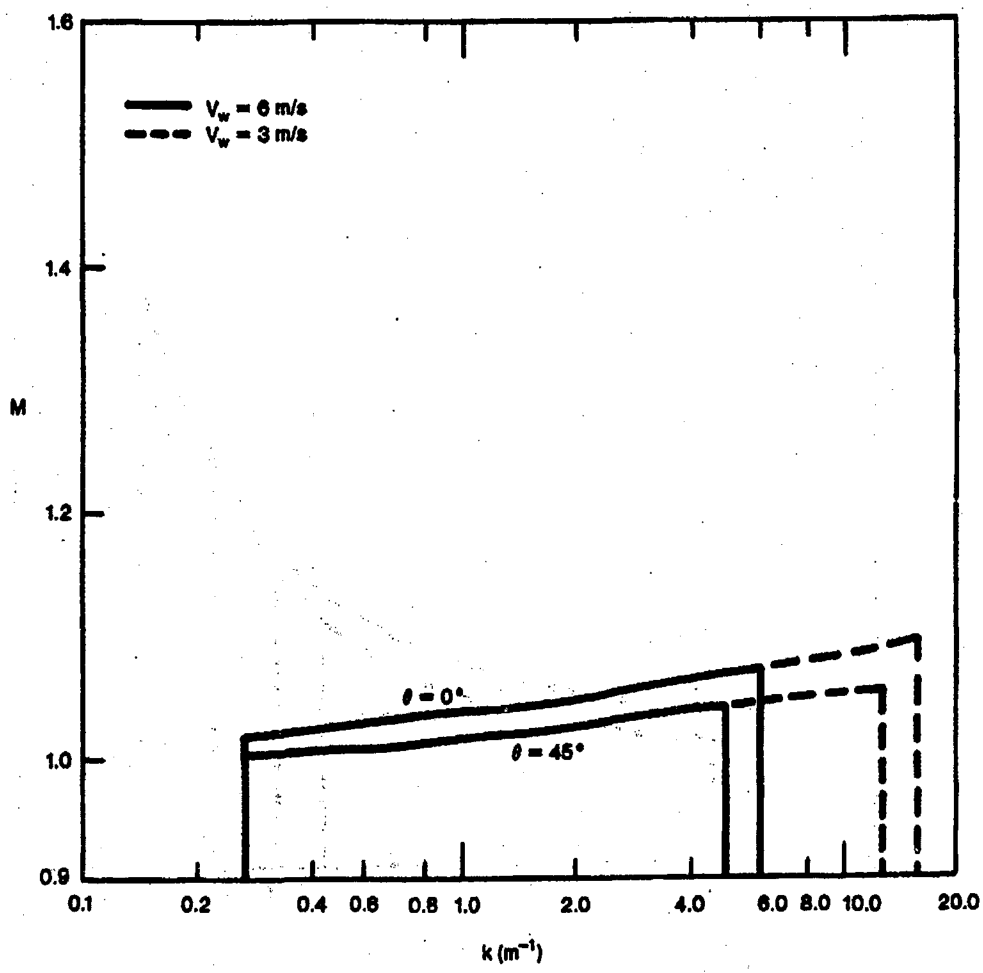

Figure 3-5. Surface wave modulation as predicted for the ENVEX1 "experiment," equation (3.17), except that $C_I = -0.33$ m/s corresponding to internal wave propagation against the wind.

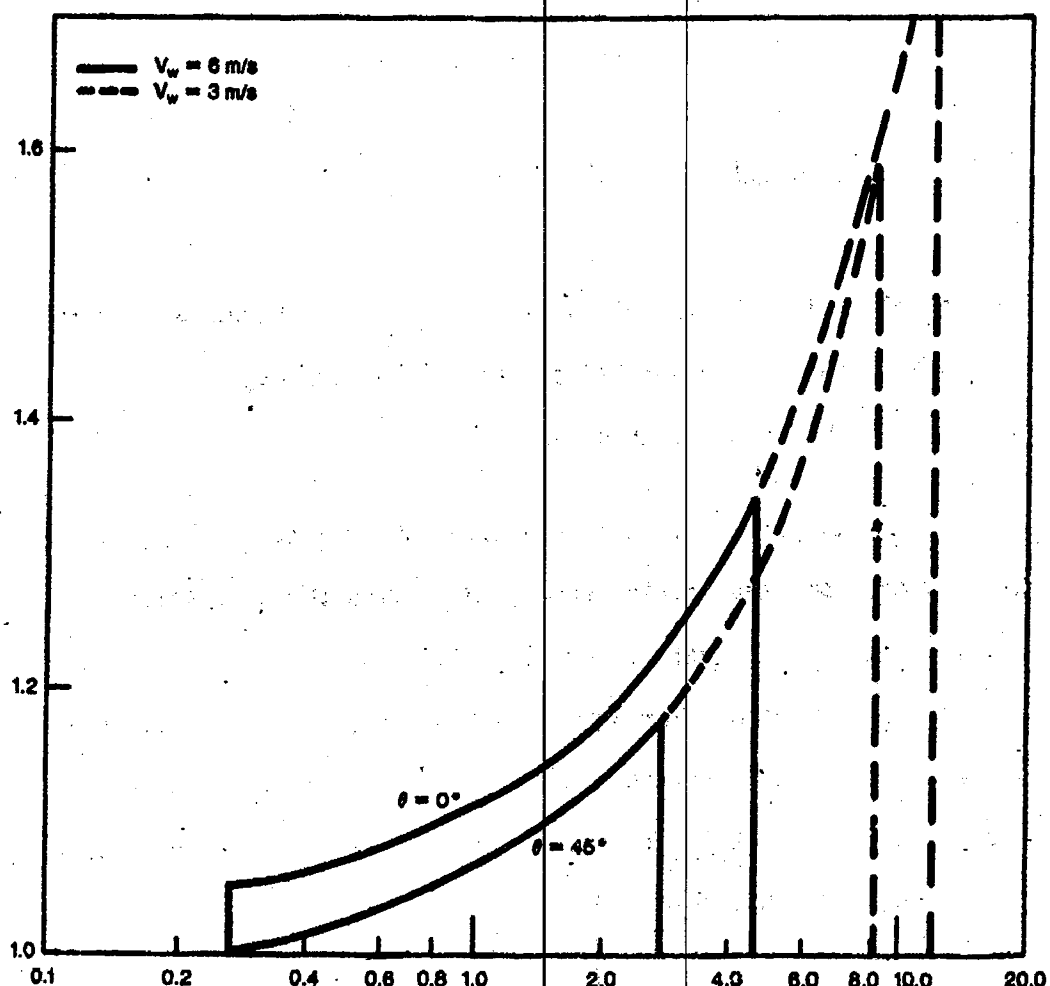

Figure 3-6. Surface wave modulation as predicted for the ENVEX2 "experiment," equation (3.18).

The variation of modulation with mixed layer thickness D [we have set N=0 in the mixed layer] is written as

$$R(D) = \frac{M \text{ (for thickness D)}}{M \text{ (for D = 10m)}} \tag{3.19}$$

The quantity is illustrated in Table 3-1 for the three sets of environmental conditions described above. The strong dependence of M on mixed layer thickness is as expected.

We are now in a position to compare the modulation M_{pert} as calculated from perturbation theory (3.9) with the modulation M obtained from exact evaluations of (3.8). We found the agreement to be surprisingly good. For example, when $|M-1| < 0.1$, our calculated values of M and M_{pert} agreed to within 0.1%. Even for substantial modulations, M and M_{pert} tended to be qualitatively similar. This is illustrated on Table 3-2.

TABLE 3-1

The variation of modulation with mixed layer thickness [see (3.19)] is shown for its three sets of environmental conditions described by equations (2.14), (3.17) and (3.18).

	R(40)	R(100)
SARSEX	0.7	0.2
ENVEX 1	0.3	0.03
ENVEX2	0.08	0.00

TABLE 3-2

The modulation M(3.8) is compared with M_{pert} (3.9), calculated from perturbation theory. The wave angle θ is taken as 0^0 here.

SARSEX

$k(m^{-1})$	KY	M	M_{pert}
0.27	3π	1.30	1.30
0.60	3π	1.50	1.40
4.6	3π	2.37	1.75
0.27	2π	0.76	0.66

ENVEX 1

$k(m^{-1})$	KY	M	M_{pert}
0.27	3π	1.03	1.03
0.60	3π	1.04	1.04
2.0	3π	1.10	1.09
4.0	3π	1.18	1.16

4.0 BRAGG WAVE MODULATION BY LONG WAVES

The calculations presented in the last section provide us with a description of the internal wave modulation of the longer wavelength portion of the gravity wave spectrum. These "carrier" waves interact with shorter surface waves in the Bragg regime, passing on the internal wave modulation. It is this, the CW^2 process, which we now investigate with a somewhat idealized model.

Our calculation is admittedly incomplete in that we have not included modulation of the "shorter of the long waves", that are strongly effected by relaxation (large β). We do not believe that this leads to serious error, however, since a large β implies small modulation.

Phillips[15] has published a description of the modulation of a short wavelength wave propagating on the surface of a dominant long wave. This analysis provides the basis for developing the CW^2 model.

Phillip's equations may be developed in the form of aseries of terms of increasing order in the ratio

(ℓ/k) and carrier slope,

where ℓ and k are wavenumbers of carrier and Bragg waves, respectively. To lowest order in these two quantities, considered here as small, the action density for Bragg waves may be obtained from (2.3) and (2.10):

$$\left[\frac{\partial}{\partial t} + \dot{\underset{\sim}{x}} \cdot \nabla_x + \dot{\underset{\sim}{k}} \; \nabla_k\right] F(\underset{\sim}{k},\underset{\sim}{x},t) = -\beta F',$$

$$F' = F - F_o,$$

$$\dot{\underset{\sim}{x}} \simeq \nabla_\omega \, \omega(k) = \underset{\sim}{C}(\underset{\sim}{k})$$

$$\dot{\underset{\sim}{k}} = - \nabla_x \, (\underset{\sim}{k} \cdot \underset{\sim}{U}_c). \tag{4.1}$$

Here $\underset{\sim}{U}_c$ is the orbital current of the carrier waves, written as a Fourier series:

$$\underset{\sim}{U}_c = \sum_{\ell}\left(\hat{\ell} \, \frac{\omega(\ell)}{2}\right) \left[a_\ell \exp\left[i(\underset{\sim}{\ell} \cdot \underset{\sim}{x} - \omega_{(\ell)} \, t)\right] + \text{C.C.}\right] \tag{4.2}$$

We consider first the case that $\beta = 0$. Integration of the ray equations gives

$$\underset{\sim}{x} \simeq \underset{\sim}{x}_o + C(\underset{\sim}{k}_o)t$$

$$k = \underset{\sim}{k}_o + \Delta \underset{\sim}{k}$$

$$\Delta \underset{\sim}{k} = -\int^t \nabla_x \left(\underset{\sim}{k} \cdot \underset{\sim}{U}_c\right) dt'$$

$$= -\sum_{\underset{\sim}{\ell}} \frac{\underset{\sim}{k} \cdot \hat{\ell}\, \underset{\sim}{\ell}\, \omega(\ell)}{2[\underset{\sim}{\ell} \cdot \underset{\sim}{c}(\underset{\sim}{k}) - \omega(\ell)]} \Big\{ a_{\underset{\sim}{\ell}} \exp[i(\underset{\sim}{\ell} \cdot \underset{\sim}{x} - \omega(\ell)t)]$$

$$+ \text{C.C.} \Big\}. \tag{4.3}$$

Using (3.7), we obtain to lowest order in $\Delta \underset{\sim}{k}$

$$F'(\underset{\sim}{k}, \underset{\sim}{x}, t) = -\Delta \underset{\sim}{k} \cdot \underset{\sim}{\nabla}_k F_o(k).$$

The Bragg modulation is then

$$M'(\underset{\sim}{k}, \underset{\sim}{x}, t) = \frac{F'(\underset{\sim}{k}, \underset{\sim}{x}, t)}{F_o(\underset{\sim}{k})}. \tag{4.4}$$

If we consider the a_{ℓ} to be Gaussian variables, the ensemble-averaged mean square modulation is

$$\langle M'^2 \rangle = \int d^2\ell \frac{\omega^2(\ell)}{[c_o(\ell) - \hat{\ell} \cdot \underset{\sim}{c}(k)]^2} \underset{\sim}{\Psi}(\ell) \, (\hat{\ell} \cdot \underset{\sim}{k})^2$$

$$\times [\hat{\ell} \cdot \nabla_k \ln F_o(\underset{\sim}{k})]^2 \tag{4.5}$$

Here $\underset{\sim}{\Psi}(\underset{\sim}{\ell})$ is the surface dsiplacement spectrum of the carrier waves. We write this as

$$\underline{\Psi}(\underline{\ell}) = M(\underline{\ell})\, \Psi_o(\underline{\ell}), \tag{4.6}$$

where $M(\underline{\ell})$ is the modulation due to IW's, as calculated in the last section, and $\underline{\Psi}_o$ is the spectrum in the absence of IW's. We have chosen the expressions (3.13) as our model for $\underline{\Psi}_o$. Also,

$$C_o(\ell) = \frac{\omega/\ell}{\ell} \tag{4.7}$$

is the phase velocity of the carrier wave.

Since the long wave spectrum is peaked in the direction $\hat{V}$ of the wind, it is permissible to set

$$(\hat{\ell} \cdot \underline{k})^2 \,[\hat{\ell} \cdot \nabla_k \,\ell n\, F_o(\underline{k})]^2 \simeq (\hat{k} \cdot \hat{V})^2 \,\alpha^2,$$

where α was introduced in (2.16). For numerical evaluation we shall again set $\alpha = \frac{9}{2}$ (a more detailed analysis would probably require a more careful determination of α). The incremental modulation of Bragg waves due to IW's is then

$$(\delta M)^2 = (\hat{k} \cdot \hat{V})^2 \,\alpha^2 \int d^2 l \,\frac{\omega^2(\ell)\, [M(\underline{\ell}) - 1]\, \underline{\Psi}_o(\underline{\ell})}{[C_o(\ell) - \hat{\ell} \cdot C(\underline{k})]^2} \tag{4.8}$$

When the β-term is dominant in (4.1) we obtain

$$M'(\underset{\sim}{k}, \underset{\sim}{x}, t) = \beta^{-1} \nabla_x(\underset{\sim}{k} \cdot \underset{\sim}{U}_c) \cdot \nabla_{\underset{\sim}{k}} \ln F_o \tag{4.9}$$

Repeating the calculation which led to (4.8) now gives

$$e\delta M)^2 = (\hat{k} \cdot \hat{V})^2 \alpha^2 \int d^2\ell \left[\left(\frac{\ell\, \omega(\ell)}{\beta}\right)\right]^2 \left[M(\underset{\sim}{\ell}) - 1\right] \underset{\sim}{\Psi}_o(\underset{\sim}{\ell}). \tag{4.10}$$

Equations (4.8) and (4.10) may be blended empirically into the single equation

$$(\delta M)^2 = (\hat{k} \cdot \hat{V})^2 \alpha^2 \int d^2\ell \, \frac{\omega^2(\ell) \left[M(\underset{\sim}{\ell}) - 1\right] \Psi_o(\underset{\sim}{\ell})}{\left[C_o(\ell) - \hat{\ell} \cdot \underset{\sim}{C}(\underset{\sim}{k})\right]^2 + \left(\frac{\beta}{\ell}\right)^2}. \tag{4.11}$$

The rms modulation δM was evaluated using (4.11) for the conditions of the SARSEX experiment (2.14), but for variable wind strength V. The result is shown in Figure 4-1 for L-band (0.2 m waves) and X-band (0.03 m waves) Braggs. It should be noted that direct modulation of L-band waves, which at low wind speeds can give a comparable contribution, has been neglected in Figure 4-1.

The L-band modulation for V = 6 m/s given in Figure 4-1 is similar to that calculated* in the SARSEX Report[3] and also is in

* Calculated as direct, not CW^2, modulation.

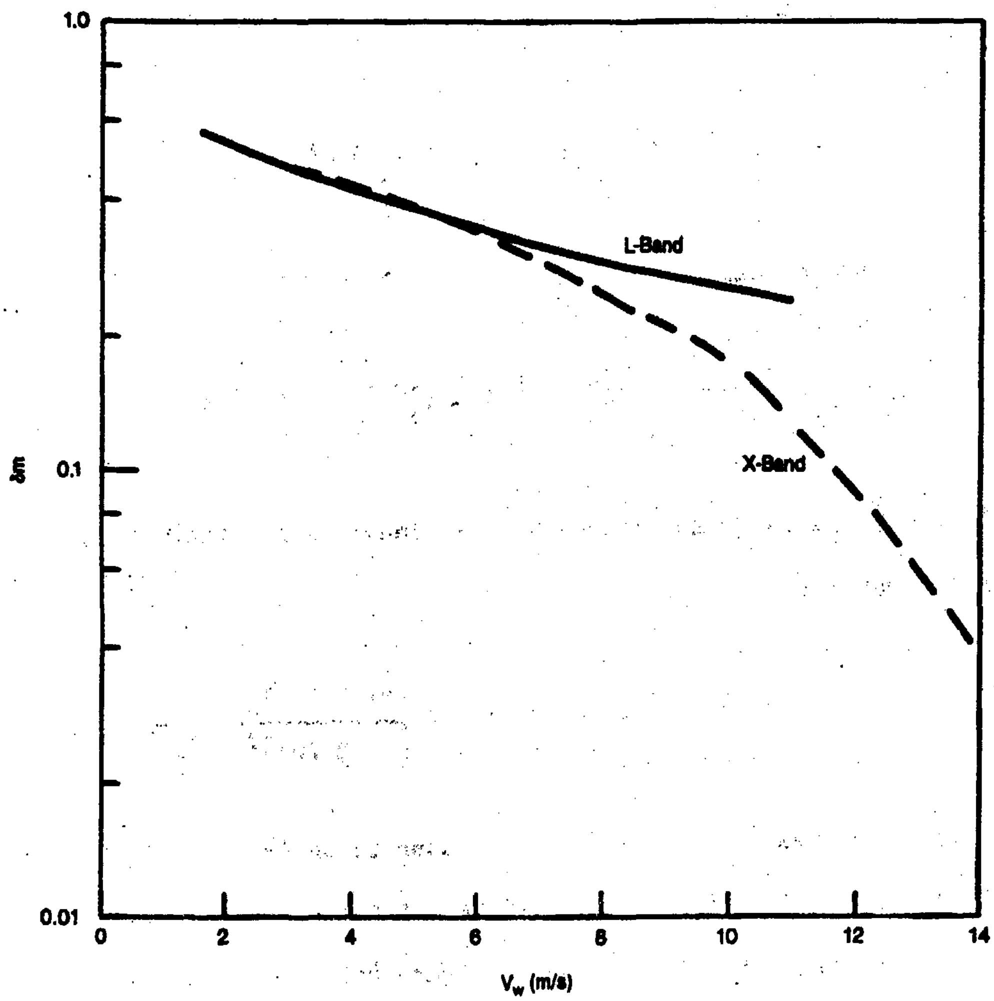

Figure 4-1. Modulation at L– and X– band as calculated from the CW^2 mechanism for internal wave G2 of the SARSEX experiment. The internal waves are propagating up-wind.

reasonable (factor of 2) agreement with the observed "wave G2" modulation. Similar agreement is also obtained with the observed X-band modulation for "G2".

For the ENVEX 1 conditions (3.17) we obtain from (4.11)

$$\delta M = 0.13. \tag{4.13}$$

It may be noted that if "bound wavelets", phase coupled to the carrier, are present, another modulation mechanism may be important. For example, the third harmonic amplitude of a Stokes wave is

$$\delta\eta = 1/3\ \ell^4 a^3 \cos[4\ell(x - C_o t)]$$

corresponding to the carrier

$$\eta = a \cos [\ell(x - C_o t)].$$

For a carrier modulation

$$M_c = \left(\frac{\delta a}{a}\right),$$

we have a fourth harmonic modulation

$$M' = 3\ M_c, \tag{4.14}$$

with increasing modulation for higher harmonics.

REFERENCES

1. Hughes, B.A., and H.L. Grant, 1978a. The Effect of Internal Waves on Surface Wind Waves 1. Experimental Measurements. J. Geophys. Res. 83, 443-454.

2. The DARPA SAR Program: Interim Report on the Georgia Strait Experiment, SAR Technology and Processing Investigations. Vol 1, 1985.

3. SARSEX Interim Report by the SARSEX Experiment Team. JHU/APL STD-R-1200, May 1985.

4. SEASAT Report, JASON/MITRE JSR-83-203, January 1985.

5. Thompson, D.R., 1985: Intensity Modulation in SAR Images of Internal Waves, JHU/APL Report.

6. Watson, K.M., B.J., West, and B.I. Cohen, 1976. Coupling of Surface and Internal Gravity Waves: A Mode Coupling Model. J. Fluid Mech 77, 185-208.

7. Dysthe, K.B. and K.P. Das, 1981, Coupling Between a Surface-Wave Spectrum and as Internal Wave: Modulational Interaction. J. Fluid Mech. 104, 483-503.

8. Watson, K.M., to be published.

9. Hughes, B.A., 1978. The Effects of Internal Waves on Surface Wind Waves 2. Theorectical Analysis. J. Geophys. Res. 83, 455-465.

10. Phillips, O.M., 1984. On the Response of Short Ocean Wave Components at Fixed Wavenumber to Ocean Current Variations. J. Phys. Oceanog. 14, 1425-1433.

11. Plant, W. J., 1982. A Relationship Between Wind Stress and Wave Slope. J. Geophys. Res. 87, 1961-1967.

12. Watson, K.M., 1986. Persistence of a Pattern of Surface Gravity Waves, J. Geophys. Res. (in process of publication).

REFERENCES (Concl'd.)

13. Tyler, G.L., C.C. Teague, R.H. Stewart, A.M. Perston, W.H. Munk, and J.W. Joy, 1974. Wave Directional Spectra from Synthetic Aperture Observations of Radio Scatter; Deep-sea Res. 21, 988-1016.

14. Mitsuyasu M., F. Tasai, T. Suhara, S. Mizuno, M. Ohkusu, T. Honda, and K. Rikushi, 1975. Observations of the Directional Spectrum of Ocean Waves using a Cloverleaf Buoy, J. Phys. Oceanog. 5, 750-760.

15. Phillips, O.M., 1981. The Dispersion of Short Wavelets in the Presence of a Dominant Long Wave; J. Fluid Mech. 107, 465-485.

DISTRIBUTION LIST

Mr. Saul Amarel
Director
DARPA/IPTO
1400 Wilson Blvd.
Arlington, VA 22209

Dr. Marv Atkins
Deputy Director, Science & Tech.
Defense Nuclear Agency
Washington, D.C. 20305

National Security Agency [2]
Attn R5: (b)(3):50 USC §402 Note
Ft. George G. Meade, MD 20755

Mr. Anthony Battista
House Armed Services Committee
2120 Rayburn Building
Washington, DC 20515

Mr. Steven Borchardt
Dynamics Technology
1815 N. Lynn Street
Suite 801
Arlington, VA 22209

Dr. Rod Butzen
Naval Ocean Systems Center
San Diego, CA 92152

Dr. Curtis G. Callan, Jr.
Princeton University
Princeton, NJ 08544

Mr. Gerald Cann
Principal Assistant Secretary
of the Navy (RES&S)
The Pentagon, Room 4E736
Washington, DC 20350

Dr. Kenneth M. Case
The Rockefeller University
New York, NY 10021

Mr. John Darrah
Sr. Scientist and Technical
Advisor
HQ Space Cmd/XPN
Peterson AFB, CO 80914

Dr. Roger F. Dashen
Institute for Advanced Study
Princeton, NJ 08540

Dr. Russ E. Davis
Scripps Institution of
Oceanography
La Jolla, CA 92093

Defense Technical Information [2]
Center
Cameron Station
Alexandria, VA 22314

CAPT Craig E. Dorman
Department of the Navy, OP-095T
The Pentagon, Room 5D576
Washington, D.C. 20350

Dr. Robert C. Duncan
DARPA
Director
1400 Wilson Boulevard
Arlington, VA 22209

Mr. John Entzminger
Director
DARPA/TTO
1400 Wilson Blvd.
Arlington, VA 22209

DISTRIBUTION LIST (Cont'd.)

Dr. Frank Fernandez
ARETE Associates
P.O. Box 350
Encino, CA 91316

Dr. J. Richard Fisher
Assistant BMD Program Manager
U.S. Army
Strategic Defense Command
P. O. Box 15280
Arlington, VA 22215-0150

(b)(3):50 USC §403(g) Section 6
P.O. Box 1925
Washington, D.C. 20505

Director [2]
National Security Agency
Fort Meade, MD 20755
ATTN: (b)(3):50 USC §402 Note

Mr. Bert Fowler
Senior Vice President
The MITRE Corporation
P.O. Box 208
Bedford, MA 01730

Mr. Richard Gasparouic
APL
John Hopkins University
Laurel, MD 20707

Dr. Larry Gershwin
NIO for Strategic Programs
P.O. Box 1925
Washington, D.C. 20505

Dr. S. William Gouse, W300
Vice President and General
Manager
The MITRE Corporation
1820 Dolley Madison Blvd.
McLean, VA 22102

Dr. William Happer
Princeton University
Princeton, NJ 08540

Dr. Edward Harper [2]
SSBN, Security Director
OP-021T
The Pentagon, Room 4D534
Washington, D.C. 20350

Dr. Donald A. Hicks [2]
Under Secretary for R&E
Office of the Secretary of
Defense
The Pentagon, Room 3E1006
Washington, D.C. 20301

Mr. R. Evan Hineman
Deputy Director for Science
& Technology
P.O. Box 1925
Washington, D.C 20505

Mr. Richard Hoglund
Senior Vice President
ORI, Inc.
1375 Piccard Drive
Rockville, MD 20850

Dr. Norden Huang
Office of Naval Research
800 N. Quincy Street
Arlington, VA 22217

Mr. Jack Kalish
Systems Planning Corporation
1500 Wilson Boulevard
Room 1542
Arlington, VA 22209

Mr. John F. Kaufmann
Deputy Director for
Program Analysis
U.S. Department of Energy
ER-31, Room F326
Washington, DC 20545

Mr. Ed Key
Vice President
The MITRE Corporation
P.O. Box 208
Bedford, MA 01730

Mr. Jerry King
RDA
P.O. Box 9695
Marina del Rey, CA 90291

MAJGEN Donald L. Lamberson
Assistant Deputy Chief of Staff
(RD&A) HQ USAF/RD, Rm. 4E334
Washington, D.C. 20330

The MITRE Corporation [3]
1820 Dolley Madison Blvd.
McLean, VA 22102
ATTN: JASON Library, W002

Mr. V. Larry Lynn
Deputy Director, DARPA
1400 Wilson Boulevard
Arlington, VA 22209

Mr. Charles Mandelbaum
Mail Stop ER-32/G-226 GTN
U.S. Department of Energy
Washington, D.C. 20545

Mr. Robert Manners
Office of Research and
Development
P.O. Box 1925
Washington, DC 20505

Mr. Walt McCandless
4608 Willet Drive
Annandale, VA 22003

(b)(3):50 USC §403(g) Secti
Deputy Director
Central Intelligence Agengy
P.O. Box 1925
Washington, D.C. 20505

Mr. John P. McTague
Deputy Director
Office of Science & Tech. Policy
Old Executive Office Building
17th & Pennsylvania Ave., N.W.
Washington, D.C. 20500

Mr. Mewson
HQ SAC/NRI
Offutt AFB
Nebraska 68113-5001

Dr. Marvin Moss [2]
Technical Director
Office of Naval Research
800 N. Quincy Street
Arlington, VA 22217

Dr. Walter H. Munk
Scripps Institute of
Oceanography
La Jolla, CA 92093

(b)(3):50 USC §403(g) Section 6
P.O. Box 1925
Washington, D.C. 20505

Director
National Security Agency
Fort Meade, MD 20755
ATTN: (b)(3):50 USC §402 Note
DDR-FANX III

DISTRIBUTION LIST (Cont'd.)

Prof. William A. Nierenberg
Scripps Institution of
Oceanography
University of California, S.D.
La Jolla, CA 92093

Dr. Robert Norwood [2]
Office of the Deputy Under
Secretary of the Army
Assistant Under Secretary
of the Army
The Pentagon, Room 2E653
Washington, D.C. 20310-0102

Mr. C. Wayne Peale
Office of Research and
Development
P.O. Box 1925
Washington, DC 20505

Dr. John Penhune
Science Applications, Inc.
MS-8
1200 Prospect Street
La Jolla, CA 92038

Mr. John Rausch [2]
NAVOPINTCEN Detachment, Suitland
4301 Suitland Road
Washington, D.C. 20390

The MITRE Corporation
Records Resources
Mail Stop W971
McLean, VA 22102

Dr. Richard Reynolds
Director
DARPA/DSO
1400 Wilson Blvd.
Arlington, VA 22209

Mr. Alan J. Roberts
Vice President & General Manager
Washington C^3I Operations
The MITRE Corporation
1820 Dolley Madison Boulevard
McLean, VA 22102

Dr. Richard S. Ruffine
OUSDRE (OS)
The Pentagon, Room 3E129
Washington, DC 20301

Dr. Phil Selwyn [2]
Technical Director
Office of Naval Technology
800 N. Quincy Street
Arlington, VA 22217

Dr. Eugene Sevin [2]
Defense Nuclear Agency
6801 Telegraph Road
Room 244
Alexandria, VA 22310

Mr. Omar Shemdin
JPL
Mail Stop 183501
4800 Oak Grove Drive
Pasadena, CA 91109

Mr. Shen Shey
Special Assistant
DARPA/DEO
1400 Wilson Blvd.
Arlington, VA 22209

Mr. Robert Shuckman
P.O. Box 8618
Ann Arbor, MI 48107

DISTRIBUTION LIST (Cont'd.)

Dr. Joel A. Snow [2]
Director
Science & Tech. Staff
U.S. DOE/ER-6
Washington, D.C. 20585

Dr. Thomas Spence
Physical Oceanography
Office of Naval Research
800 N. Quincy Street
Arlington, VA 22217

COMO William O. Studeman
Director of Naval Intelligence
Office of Naval Intelligence
Navy Department (OP-009)
Washington, D.C. 20310

Mr. Alexander J. Tachmindji
Senior Vice President & General Manager
The MITRE Corporation
P.O. Box 208
Bedford, MA 01730

Dr. Vigdor Teplitz
ACDA
320 21st Street, N.W.
Room 4484
Washington, D.C. 20451

Mr. Anthony J. Tether
Director
DARPA/STO
1400 Wilson Blvd.
Arlington, VA 22209

Mr. Marshall Tulin
Dept. of Mechanical Engineering
University of California
Santa Barbara, CA 93106

Dr. John F. Vesecky
Stanford University
Stanford, CA 94305

The Honorable James P. Wade, Jr.
Assistant Secretary of Defense
Acquisition & Logistics
The Pentagon, Room 3E1014
Washington, DC 20301

Dr. Kenneth M. Watson
Scripps Institution of Oceanography
La Jolla, CA 92093

Mr. Robert Winokur
Assistant Technical Director for Ocean Science
Office of Naval Research
800 N. Quincy Street
Arlington, VA 22217

LTCOL Simon Peter Worden
Strategic Defense Initiative Organization
1717 H. Street, Rm. 416
Washington, D.C. 20301

Dr. Gerold Yonas [2]
Strategic Defense Initiative Organization
Office of the Secretary of Defense
The Pentagon
Washington, DC 20301-7100

Mr. Leo Young
OUSDRE (R&AT)
The Pentagon, Room 3D1067
Washington, D.C. 20301-3081

DISTRIBUTION LIST (Concl'd.)

Dr. Fredrik Zachariasen
California Institute of
Technology
Pasadena, CA 91125

Mr. Charles A. Zraket
Executive Vice President
The MITRE Corporation
P.O. Box 208
Bedford, MA 01730